

Cite this: *Catal. Sci. Technol.*, 2020, 10, 8203

The direct synthesis of hydrogen peroxide using a combination of a hydrophobic solvent and water†

Adeeba Akram,^a Greg Shaw,^a Richard J. Lewis,^a Marco Piccinini,^a David J. Morgan,^a Thomas E. Davies,^a Simon J. Freakley,^b Jennifer K. Edwards,^a Jacob A. Moulijn^a and Graham J. Hutchings^{a*}

The direct synthesis of hydrogen peroxide (H₂O₂) has been studied using a solvent system comprising a hydrophobic alcohol (decan-1-ol) and water. It is demonstrated that, with the optimum combination of solvent and catalyst the contribution of H₂O₂ degradation pathways can be minimised to achieve industrially acceptable H₂O₂ concentrations under moderate conditions. This is achieved through the use of a catalyst that is retained by the organic component and the extraction of synthesised H₂O₂ into the aqueous phase, consequently limiting contact between the synthesised H₂O₂, catalyst and reactant gases, resulting in an improved selectivity towards H₂O₂. Investigation of the reaction parameters provides an insight into the proposed solvent system, and optimised conditions to produce H₂O₂ from molecular H₂ and O₂ have been identified. Through this optimisation H₂O₂ concentrations up to 1.9 wt% have been achieved *via* sequential gas replacement experiments.

Received 9th June 2020,
Accepted 15th October 2020

DOI: 10.1039/d0cy01163k

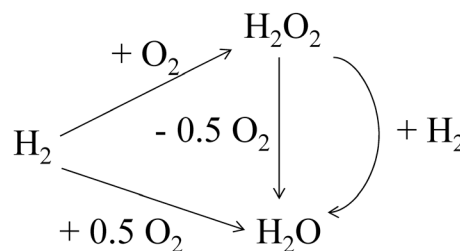
rsc.li/catalysis

Introduction

The direct synthesis of hydrogen peroxide (H₂O₂) from molecular hydrogen and oxygen offers an attractive alternative to the current means of production, the anthraquinone oxidation or in-direct process. The direct route to H₂O₂ has been carried out in a wide range of reaction media, including water.^{1–9} For many applications the most convenient solvent for the reaction would be water as it is readily available, non-toxic, non-flammable and completely miscible with H₂O₂. Indeed a large number of industrial processes utilise aqueous H₂O₂, in particular for application as a bleaching agent in the pulp and textiles sector (accounting for nearly 50% of annual usage¹⁰) H₂O₂ diluted in water is favoured.¹¹ However, a major drawback of using H₂O as a solvent is the low solubility of reagent gases H₂ and O₂, (1.62 mg L⁻¹ and 40 mg L⁻¹ respectively, at room temperature)¹² which has been shown to limit H₂O₂ synthesis rates, compared to that observed when using alcohol/water co-solvent systems.^{1,2} To overcome these limitations solvents other than water have been investigated including supercritical CO₂^{13–16} and halogenated solvents^{17–19} as well as short chain alcohols,^{9,20,21} with Paunovic *et al.*²² providing a comprehensive study on the role of the co-solvent

in the direct synthesis reaction. It has been reported that the rate of H₂O₂ production in short chain alcohols is much higher than that in aqueous media due to higher gas solubility.^{20,23} The solubility of H₂ in short chain alcohols, in particular methanol, has been reported to be 4–5 times higher than in water whereas that of O₂ may increase up to eightfold.^{24,25} Furthermore, additional studies have reported that using a methanol co-solvent can lead to the suppression of H₂O₂ decomposition activity, likely due to the ability of methanol to act as a hydroxyl radical scavenger.²⁶

Despite this approach, the presence of subsequent reactions in the H₂O₂ direct synthesis process (Scheme 1) suggests that it will remain challenging to achieve high H₂O₂ concentrations, due to the thermodynamically favoured H₂O₂ degradation pathways (hydrogenation and decomposition). Typically, these unwanted reaction pathways have been inhibited through the use of a combination of sub-ambient reaction temperatures,²⁷ acidic promoters,^{28–30} halide



Scheme 1 Reaction pathways associated with the direct synthesis of H₂O₂ from H₂ and O₂.

^a Cardiff Catalysis Institute, School of Chemistry, Cardiff University, Main Building, Park Place, Cardiff, CF10 3AT, UK. E-mail: hutch@cardiff.ac.uk

^b Department of Chemistry, University of Bath, Claverton Down, Bath, BA2 7AY, UK

† Electronic supplementary information (ESI) available. See DOI: 10.1039/d0cy01163k

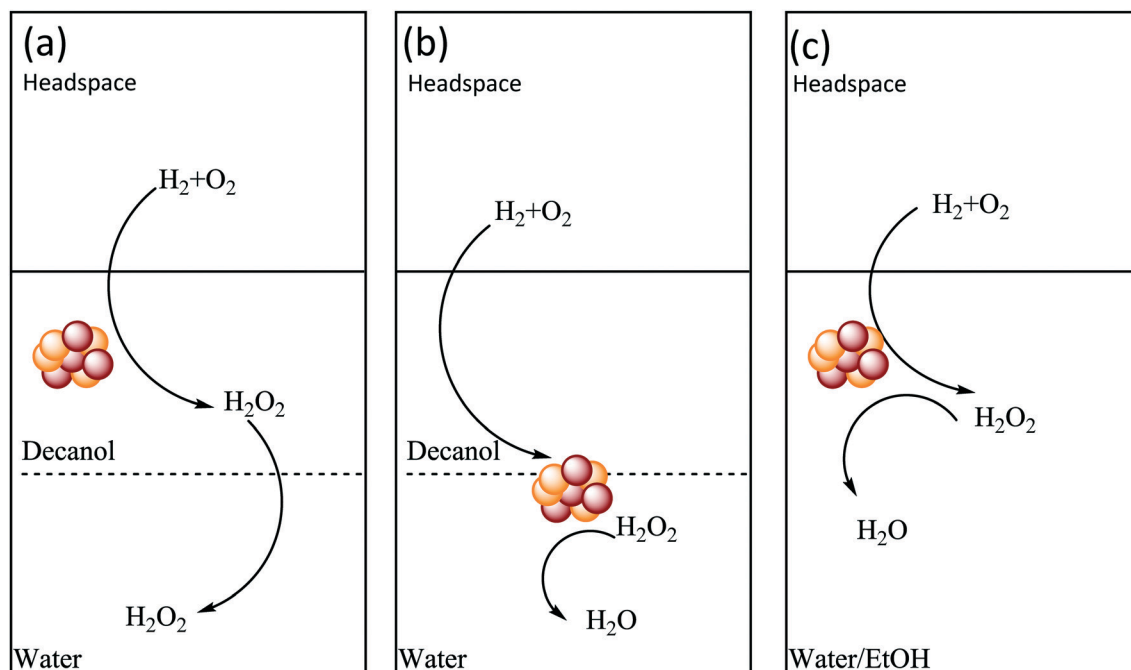


stabilizing agents^{31,32} (with obvious drawbacks associated with reactor corrosion and the need for their down-stream removal) or complicated catalyst design, such as pre-treatment of catalyst supports prior to metal immobilisation³³ or sequential heat treatment cycles.³⁴ While a growing number of catalysts have been reported that are capable of achieving high H₂O₂ selectivity,^{33–35} in the absence of stabilizing agents, the consecutive reaction pathways still prohibit the production of H₂O₂ concentrations on an industrial scale, with H₂O₂ concentrations between 0.6–1.8 wt% typically produced in initial stages of the industrial process, prior to concentration and shipping.³⁶

With the first order dependence of H₂O₂ synthesis on H₂ partial pressure,³⁷ increasing H₂ concentration at the catalyst surface through application of a short chain alcohol as solvent or increasing reaction pressure (which is not attractive for a commercial process) can inherently be related to a proportional increase in the rate of H₂O₂ production. A bi-phasic solvent system consisting of long chain alcohols and water could provide both high solubility of gases and the ability to extract H₂O₂ into the aqueous phase under moderate conditions. Ideally in this system, the catalyst and gases will be held in the organic phase where H₂O₂ will be produced and subsequently extracted *in situ* into the aqueous phase due to the higher solubility of H₂O₂ in water than the organic solvent. The use of a bi-phasic solvent system has the potential to lead to enhanced selectivity towards H₂O₂, through minimising contact time between H₂O₂, the catalyst and reactant gases, which in turn leads to a reduction in the subsequent H₂O₂ degradation reactions and, thus, an

increase in H₂O₂ concentration. Indeed similar approaches have been recently been reported for the production of H₂O₂ *via* photocatalytic processes^{38–40} as well as in the biomass conversion literature, where bi-phasic solvent systems often lead to higher product yields than with mono-phasic aqueous systems due to the higher solubility of products in the organic phase.⁴¹ Furthermore, the use of multi-phasic systems has been well established in processes that utilise homogeneous catalysts.^{42,43} In the case of H₂O₂ synthesis, when selecting a suitable candidate for the organic phase two key features are required, an ability to produce H₂O₂ in the solvent, and a low water solubility. In order to narrow down the search for a suitable organic solvent only primary alcohols were considered in this study. Water was selected as the co-solvent due to it being low cost, readily available and its full miscibility with H₂O₂.

The choice of the catalyst support is also an important parameter to consider, with the ability of the catalyst to be retained in the hydrophobic solvent, during the course of the reaction, crucial to inhibiting H₂O₂ degradation. In this optimum scenario (Scheme 2a) the contact between catalyst and reagent gases would be maximized, while also isolating the formed H₂O₂ and inhibiting degradation pathways. On the other hand, the use of a catalyst that is retained primarily in the aqueous phase (Scheme 2b), or indeed the use of a single phase solvent system, such as water/ethanol⁴⁴ or water/methanol,^{35,45,46} which are both commonly studied in the literature, (Scheme 2c) would not limit contact between synthesised H₂O₂, catalyst and reagent gases, leading to increased rates of H₂O₂ degradation. With the application of



Scheme 2 The effect of solvent and catalyst support on promoting H₂O₂ selectivity in (a) a non-miscible solvent system where the catalyst is retained in the organic component of the solvent, (b) a non-miscible solvent system where the catalyst is retained in the aqueous component of the solvent and (c) a completely miscible solvent system.



stabilizing agents, to inhibit catalytic degradation of H₂O₂, typical in these miscible solvent systems.

This paper outlines the investigation of the direct synthesis of H₂O₂ based on the described hydrophobic alcohol and water solvent system. Reaction parameters have been varied, namely water concentration, catalyst support, solvent mass and reaction time to deduce the feasibility of the outlined solvent system.

Experimental

Preparation of AuPd supported catalysts by wet impregnation

AuPd bimetallic catalysts were prepared *via* a wet co-impregnation onto a range of supports; Darco G60 carbon (C), Aerioxide TiO₂ (Degussa, Aerioxide, P25), SiO₂ and CeO₂. The standard preparation of 2.5 wt% Au–2.5 wt% Pd supported catalyst is described as follows (all quantities stated are per 1 g of catalyst). PdCl₂ (0.0417 g, Sigma Aldrich) was added to HAuCl₄·3H₂O (2.04 mL, 12.25 mg mL⁻¹, Strem Chemicals). The solution was stirred and heated (80 °C) until the PdCl₂ dissolved completely to form a homogeneous solution. The appropriate support (0.95 g) was added to the solution and stirred until a paste was formed. The resultant material was dried in an oven (110 °C, 16 h) before being ground and calcined in static air (400 °C, 3 h, 20 °C min⁻¹).

Characterisation

The volumetric Karl Fischer method was performed using a TitroLine® 7500 KF volumetric Karl Fischer titrator where the titrating agent was accurately added through a piston burette. The standard procedure for each titration was as follows. The burette was filled with the titrating agent (Hydranal®-Composite 5). The working medium (Hydranal®-CompoSolver E) was added to the titration vessel, which was titrated to dryness with the titrating agent. The organic solvent sample was added (between 0.1–1.0 g depending on expected water concentration) and the sample was titrated with the titrating agent to determine the water concentration.

¹H NMR spectra were recorded on a Bruker Ultrashield 500 MHz spectrometer, using a H₂O solvent suppression program. Filtered solvent (0.7 mL) was added to an NMR tube containing D₂O (0.1 mL).

Investigation of the bulk structure of the crystalline materials was carried out using a (θ - θ) PANalytical X'pert Pro powder diffractometer using a Cu K α radiation source, operating at 40 KeV and 40 mA. Standard analysis was carried out using a 40 min run with a back filled sample, between 2 θ values of 10–80°. Phase identification was carried out using the International Centre for Diffraction Data (ICDD).

X-ray photoelectron spectroscopy (XPS) analyses were made on a Kratos Axis Ultra DLD spectrometer. Samples were mounted using double-sided adhesive tape and binding energies were referenced to the C (1s) binding energy of adventitious carbon contamination that was taken to be 284.7 eV. Monochromatic AlK α radiation was used for all

measurements; an analyser pass energy of 160 eV was used for survey scans while 40 eV was employed for detailed regional scans. The intensities of the Au (4f) and Pd (3d) features were used to derive the Au/Pd surface ratios.

To allow for quantification of total metal loading catalysts were digested *via* an *aqua-regia* assisted, microwave digestion method using a Milestone Connect Ethos UP microwave with an SK15 sample rotor. Digested samples were analysed using an Agilent 7900 ICP-MS equipped with I-AS auto-sampler. All samples were diluted by a factor of 10 using HPLC grade H₂O (1% HNO₃ and 0.5% HCl matrix). All calibrants were matrix matched and measured against a five-point calibration using certified reference materials purchased from Perkin Elmer and certified internal standards acquired from Agilent.

Direct synthesis of H₂O₂

Catalyst testing was performed using a Parr Instruments stainless steel autoclave which had a nominal volume of 100 mL and a maximum working pressure of 14 MPa. The autoclave was equipped with an overhead stirrer (0–2000 rpm) and provision for measurement of temperature and pressure. To test the direct synthesis of H₂O₂, the autoclave was typically charged with catalyst (0.01 g) and saturated decan-1-ol (0.39 g H₂O and 8.11 g decan-1-ol). The charged autoclave was purged three times with 5% H₂/CO₂ (100 psi) and then filled with 5% H₂/CO₂ (420 psi) and 25% O₂/CO₂ (160 psi) to give a H₂:O₂ ratio of 0.5 and a total working pressure of 580 psi, with no continual introduction of gas. The reaction mixture was allowed to stabilise at the desired temperature (25 °C) after which stirring commenced (1200 rpm) and experiments were carried out for 30 minutes, unless stated otherwise. H₂O₂ yield was determined by titrating all of the final solution (unless stated otherwise) with acidified Ce(SO₄)₂. The Ce(SO₄)₂ solutions were standardised against (NH₄)₂Fe(SO₄)₂·6H₂O using ferroin as an indicator. These reaction conditions were systematically varied in this study.

In this paper, results have been primarily obtained with saturated (with water) decan-1-ol, with the amount of hydrogen peroxide discussed in terms of the theoretical H₂O₂ concentration in water (wt%). The H₂O₂ concentration is expressed assuming facile separation of decan-1-ol and water can be achieved, with no H₂O₂ retained in the organic solvent.

Time-on-line analysis for the direct synthesis of H₂O₂

An identical procedure to that outlined above for the direct synthesis of H₂O₂ is followed for the desired reaction time. It should be noted that individual experiments are carried out and the reaction mixture is not sampled on-line.

Gas replacement experiments for the direct synthesis of H₂O₂

An identical procedure to that outlined above for the direct synthesis of H₂O₂ is followed for a reaction time of 0.5 h. After this, stirring is stopped and the reactant gas mixture is vented prior to replacement with the standard pressures of



5% H₂/CO₂ (420 psi) and 25% O₂/CO₂ (160 psi). The reaction is then stirred (1200 rpm) for a further 0.5 h.

Degradation of H₂O₂

Catalytic activity towards H₂O₂ degradation was determined in a similar manner to the direct synthesis activity of a catalyst. The autoclave was typically charged with catalyst (0.01 g) and reaction solution (0.39 g 4 wt% H₂O₂ and 8.11 g organic solvent). The charged autoclave was purged three times with 5% H₂/CO₂ (100 psi) and then filled with 5% H₂/CO₂ (420 psi). The reaction mixture was allowed to stabilise at the desired temperature (25 °C) after which stirring commenced (1200 rpm) and experiments were carried out for 30 minutes. H₂O₂ degraded was determined by titrating all of the final solution with acidified Ce(SO₄)₂. The Ce(SO₄)₂ solutions were standardised against (NH₄)₂Fe(SO₄)₂·6H₂O using ferroin as an indicator. Catalytic activity towards H₂O₂ degradation is reported herein in terms of rate (mol_{H₂O₂} kg_{cat}⁻¹ h⁻¹) to better allow for comparison to the literature and accounts for hydrogenation and decomposition pathways.

Note: within this work reactant gases have been diluted with CO₂ to ensure that at no time do mixtures of H₂ and O₂ enter the explosive region (4–94 mol%).

Results and discussion

Within this study we evaluate the catalytic performance of a range of previously studied supported AuPd catalysts prepared by a wet co-impregnation methodology, (5% AuPd/C,³³ 5% AuPd/TiO₂,⁶ 5% AuPd/CeO₂ (ref. 47) and 5% AuPd/SiO₂ (ref. 27)) (actual metal loading, as determined by *aqua-regia* assisted microwave digestion reported in Table S.1†) towards H₂O₂ synthesis, using a solvent system consisting of a hydrophobic alcohol and water. We aim to address H₂O₂ selectivity through minimizing contact between catalyst and the synthesised H₂O₂, with the choice of solvent ensuring the former is preferentially retained in the hydrophobic alcohol while the latter extracted into the aqueous phase.

We have previously demonstrated that catalytic selectivity of the materials studied within this work correlates strongly with the surface charge of the support, with catalysts synthesised on supports such as C and SiO₂, which have low isoelectric points, offering the greatest rates of H₂O₂ synthesis.⁴⁸ Although other parameters such as nanoparticle dispersion,⁴⁹ the degree of alloying⁵⁰ and Pd oxidation state^{51,52} are clearly also strongly related to catalytic performance.

With this in mind we initially investigated the as-prepared catalysts *via* XRD (Fig. S.1†), with reflections observed at 38, 44, 66 and 78° corresponding to Au (111), (200) (220) and (311) planes in all samples, in addition to reflections at 65 and 79° corresponding to the Pd (220) and (311) planes observed in the AuPd/SiO₂ catalyst. This is indicative of the supported nanoparticles generally being large or poorly dispersed. This is perhaps unsurprising, with catalysts prepared *via* a wet-impregnation procedure well known to display a bimodal distribution of nanoparticle size.⁵³ Indeed

detailed STEM-XEDS analysis of oxide supported AuPd nanoparticles has previously revealed a distinct relationship between particle size and elemental composition, with larger nanoparticles found to be Au-rich, while smaller nanoparticles are Pd-rich.⁵⁴ In a similar manner we have demonstrated that analogously prepared carbon supported catalysts also adopt a size dependent nanoparticle-composition. However, unlike with catalysts prepared on oxide supports, which adopt a Au-core Pd-shell morphology after exposure to an oxidative heat treatment, analogous catalysts prepared on carbon have been found to maintain the random alloy morphology observed prior to calcination.⁵⁵

We⁵⁵ and others^{56,57} have extensively studied the synergistic effect achieved through the incorporation of Au into supported Pd catalysts with the reduction in contiguous Pd ensembles often attributed as the cause for the enhanced catalytic performance observed compared to monometallic analogues. Further studies have highlighted the role Au plays in electronically modifying Pd, with Au incorporation suppressing O–O bond cleavage, inhibiting the formation of H₂O, as well as promoting H₂O₂ desorption through weakening the interaction between the as-synthesised H₂O₂ and the catalyst surface.^{58–60} In particular the formation of Au-core Pd-shell nanoparticle morphology, commonly adopted upon the calcination of AuPd nanoparticles supported on oxide supports, has been widely reported to result in enhanced catalytic performance. Analysis of the various AuPd catalyst (Table S.2 and Fig. S.2†) *via* XPS reveals that the observed Pd: Au surface atomic ratios for the oxide supported catalysts are markedly higher than the nominal compositions, with these observations consistent with a Au-core Pd-shell nanoparticle morphology. By comparison, the Au: Pd surface ratio for the carbon supported catalyst is more in keeping with the formation of a homogeneous alloy, again with this aligning well with our previous studies.^{54,55}

The as-prepared catalysts were investigated for their affinity to be retained in a hydrophobic solvent. Samples were added to a solvent with two distinct phases, decan-1-ol and water. After vigorous shaking it was observed (Fig. 1) that only the 5% AuPd/C remained in the alcohol phase, whereas the analogous TiO₂, CeO₂ and SiO₂ supported catalysts were predominately present in the aqueous phase. These results are not unexpected as TiO₂, CeO₂ and SiO₂ are more polar than C.

We have previously investigated the ability of these catalysts to synthesise H₂O₂ under conditions optimised to promote H₂O₂ stability, namely the use of a methanol–water solvent system and sub-ambient temperature¹ (see Table S.3† for H₂O₂ synthesis and degradation under these conditions). Subsequently we have investigated the catalytic activity of these bi-metallic catalysts towards H₂O₂ degradation using a water/decan-1-ol solvent system, (Table S.4†) with the 5% AuPd/C catalyst demonstrating significantly lower rates of H₂O₂ degradation compared to oxide supported analogues, presumably due to the greater retention of the catalyst in the organic phase and decreased contact between catalyst and synthesised H₂O₂.



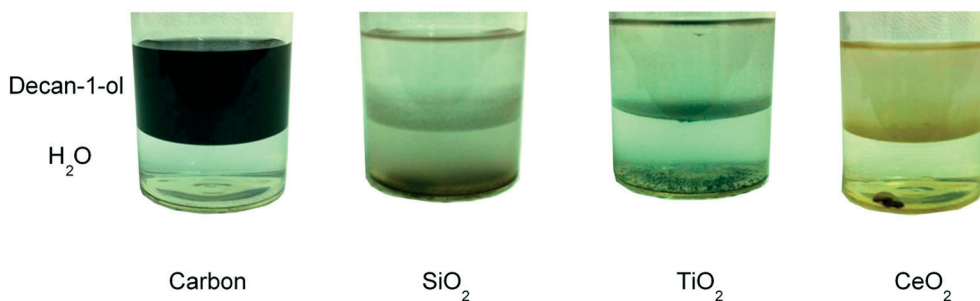


Fig. 1 Images of 5% AuPd/supported catalysts (carbon, SiO₂, TiO₂ and CeO₂) in a two-phase solvent system consisting of decan-1-ol (top layer) and water (bottom layer).

We have previously reported that the 5% AuPd/C catalyst, offers a reasonably high activity towards H₂O₂ synthesis using a methanol–water co-solvent system under reaction conditions that are similar to those reported herein (98 mol_{H₂O₂} kg_{cat}⁻¹ h⁻¹).³

We next investigated the efficacy of the 5% AuPd/C catalyst towards the direct synthesis of H₂O₂ in a range of straight chain alcohols (containing no aqueous co-solvent) as solvent (Table 1). Previous studies investigating the direct synthesis of H₂O₂ in short chain alcohol solvents have typically utilised acidic or halide promoters (or a combination thereof) to achieve high selectivity towards H₂O₂.^{20,61} Under our reaction conditions, where no halide or acidic promoters are utilised, low concentrations of H₂O₂ were produced in all alcohols studied with H₂O₂ concentration decreasing with increasing carbon chain length, with this possibly resulting from a number of factors including (i) decreased O₂ solubility as a function of alcohol carbon-chain length,⁶² or (ii) increasing H₂O₂ degradation due to improved H₂ solubility.²⁴ The ability to produce H₂O₂ therefore strongly depends on the overall rate of mass transfer of gaseous reactants to the catalyst surface. Thus, the decreasing concentration of observed H₂O₂ is likely to be due to a mixture of both chemical and physical properties of the solvent such as higher viscosity and surface tension as the alcohol carbon chain length increases. A larger pressure drop of the reagent gases was also observed during reaction (Table S.5†), indicating increased solubility of reactant gases, although the possibility for increased solubility of the CO₂ diluent should not be ruled out, in keeping with observations by Francesconi *et al.*²⁴ and Wainwright *et al.*²⁵ who have shown that H₂ solubility in the C1–4 primary alcohol series increases

with carbon chain length and therefore it is reasonable to expect H₂ to dissolve better in decan-1-ol rather than methanol.

Another important consideration when selecting the organic solvent was the requirement to have low water solubility in the alcohol phase in order to create a bi-phasic solvent system, which would allow for ease of separation of H₂O₂. Table 1 shows that the use of a methanol-only solvent results in the highest H₂O₂ concentration (250 μmol). However, due to the complete miscibility of methanol with water, it is not a suitable solvent choice for this investigation. Higher carbon chain alcohols (>C6) have lower water solubility and the addition of excess water can create a bi-phasic solvent system.⁶³ The saturation point of the alcohols in water has been determined experimentally by Karl Fischer titration (Table 2). As decan-1-ol was determined to have the lowest water solubility (46 g_{H₂O} kg_{decan-1-ol}⁻¹), while also allowing for the formation of H₂O₂, it was chosen as a suitable solvent for the hydrophobic solvent layer of the proposed two-phase system. Furthermore, decan-1-ol has been shown to be stable under reaction conditions by NMR analysis (Fig. S.3†).

The effect of solvent composition on the direct synthesis of H₂O₂, by varying the water concentration in decan-1-ol, from 0 to 590 g_{H₂O} kg_{decan-1-ol}⁻¹, was investigated (Fig. 2), while maintaining all other reaction variables, including total solvent mass which was maintained at 8.5 g. Increasing water content is observed to lead to an increase in H₂O₂ concentration, with the maximum H₂O₂ concentration (0.17 wt%) being observed at the saturation point of decan-1-ol; 46 g_{H₂O} kg_{decan-1-ol}⁻¹ (0.39 g of H₂O and 8.11 g of decan-1-ol). This is ascribed to the inhibition of H₂O₂ degradation (*via* hydrogenation and decomposition pathways) through the

Table 1 Catalytic activity of 5% AuPd/C towards H₂O₂ synthesis as a function of alcohol chain length and the solubility of water in various alcohols

Solvent	H ₂ O ₂ productivity (mol _{H₂O₂} kg _{cat} ⁻¹ h ⁻¹)	[H ₂ O ₂] (wt%)	H ₂ O ₂ produced (μmol)	H ₂ O solubility ^a (g _{H₂O} kg _{solvent} ⁻¹)
Water	10	0.016	50	—
Methanol	50	0.094	250	—
Propan-1-ol	32	0.063	160	—
Butan-1-ol	26	0.030	130	—
Hexan-1-ol	4.4	0.008	22	94
Octan-1-ol	1.4	0.003	7	53
Decan-1-ol	0.8	0.002	4.2	46

H₂O₂ synthesis reaction conditions: 5% AuPd/C (0.01 g), total pressure (580 psi), H₂/O₂ (0.5), 1200 rpm, 8.5 g total solvent, 25 °C, 30 min (note: no H₂O added). ^a As measured by Karl Fisher titration.



Table 2 The effect of total reaction pressure on catalytic activity towards H_2O_2 formation using a bi-phasic $\text{H}_2\text{O}/\text{decan-1-ol}$ solvent system using a 5% AuPd/C catalyst

Entry	Total pressure/psi	$[\text{H}_2\text{O}_2]/\text{wt}\%$	H_2O_2 productivity/ $\text{mol}_{\text{H}_2\text{O}_2} \text{kg}_{\text{cat}}^{-1} \text{h}^{-1}$
1 ^a	580	0.17	3.3
2	580	0.45	2.0
3	700	0.81	3.7

H_2O_2 synthesis reaction conditions: 5% AuPd/C (0.02 g), total pressure (580–700 psi), H_2/O_2 (0.5), 1200 rpm, 4 g total solvent ($39 \text{ g}_{\text{H}_2\text{O}} \text{kg}_{\text{decan-1-ol}}^{-1}$), 25 °C, 30 min. ^a Non-optimised reaction conditions. 5% AuPd/C (0.01 g), total pressure (580 psi), H_2/O_2 (0.5), 1200 rpm, 8.5 g total solvent ($39 \text{ g}_{\text{H}_2\text{O}} \text{kg}_{\text{decan-1-ol}}^{-1}$), 25 °C, 30 min.

separation of H_2O_2 from the catalyst and the *in situ* formation of carbonic acid in the aqueous phase, through solvation of the CO_2 gaseous diluent, with the improved stability of H_2O_2 under acidic conditions well known.^{64,65} Indeed similar improvements in H_2O_2 concentrations have been observed through the introduction of water into methanol solvent systems.^{1–3} The sharp increase in the H_2O_2 concentration up to $46 \text{ g}_{\text{H}_2\text{O}} \text{kg}_{\text{decan-1-ol}}^{-1}$ demonstrates that the presence of water has a significant effect on the concentrations of H_2O_2 that can be achieved over the 5% AuPd/C catalyst. On further increasing the water content, to form a bi-phasic solvent, there was little effect on the H_2O_2 concentration up to $120 \text{ g}_{\text{H}_2\text{O}} \text{kg}_{\text{decan-1-ol}}^{-1}$. Increasing H_2O content beyond $150 \text{ g}_{\text{H}_2\text{O}} \text{kg}_{\text{decan-1-ol}}^{-1}$ lead to a significant decrease in H_2O_2 concentration, with this attributed to a combination of decreased H_2 availability, with increasing water content, and the inability of the decan-1-ol phase to retain the totality of the catalyst, leading to increased contact between catalyst and synthesised H_2O_2 and in turn increased H_2O_2 degradation.

With water concentrations above $120 \text{ g}_{\text{H}_2\text{O}} \text{kg}_{\text{decan-1-ol}}^{-1}$ (1 g H_2O and 7.5 g decan-1-ol) it was possible to separate the

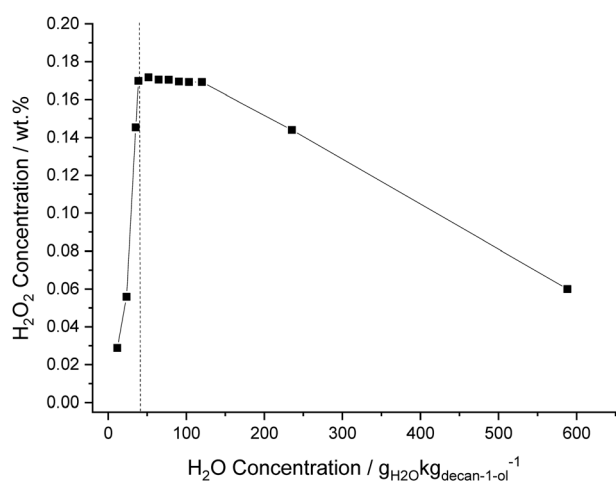


Fig. 2 The effect of H_2O content in a $\text{H}_2\text{O}/\text{decan-1-ol}$ solvent system on the direct synthesis of H_2O_2 . H_2O_2 concentration (black squares). H_2O_2 synthesis reaction conditions: 5% AuPd/C (0.01 g), total pressure (580 psi), H_2/O_2 (0.5), 1200 rpm, 8.5 g total solvent (decan-1-ol + water), 25 °C, 30 min. (—) H_2O saturation point of decan-1-ol.

water and decan-1-ol in order to directly calculate the H_2O_2 concentration in the aqueous phase. Comparing these extracted H_2O_2 concentrations with the results obtained from titrating the entire decan-1-ol and water solvent are shown in Fig. 3. When $120 \text{ g}_{\text{H}_2\text{O}} \text{kg}_{\text{decan-1-ol}}^{-1}$ (1 g H_2O and 7.5 g decan-1-ol) and $235 \text{ g}_{\text{H}_2\text{O}} \text{kg}_{\text{decan-1-ol}}^{-1}$ (2 g H_2O and 6.5 g decan-1-ol) were added the difference between the results obtained through analysis of the total reaction solution or the aqueous phase only is 16–17%, suggesting that at low H_2O extraction of H_2O_2 is incomplete. The difference between the two measures of H_2O_2 content was subsequently decreased to 6% when the water phase was more easily separated from the decan-1-ol at $590 \text{ g}_{\text{H}_2\text{O}} \text{kg}_{\text{decan-1-ol}}^{-1}$ (5 g H_2O and 3.5 g decan-1-ol). This indicates that the efficiency of separating the two solvents will be a critical step to maintaining the formed H_2O_2 concentrations. All preceding results were obtained from titrating the whole solvent mixture to allow for accurate determination of H_2O_2 concentrations.

The solvent system was next investigated for its ability to suppress H_2O_2 degradation, under an atmosphere of 5% H_2/CO_2 (Fig. 4). Reactions were carried out with increasing amounts of pre-formed 4 wt% aqueous H_2O_2 added to decan-1-ol; from a saturated decan-1-ol solution (0.39 g) to a truly bi-phasic solvent system (3.0 g), keeping the total solvent mass constant (8.5 g). When 0.39 g of 4 wt% H_2O_2 , was added to decan-1-ol (8.11 g), to achieve a saturated decan-1-ol solution, a degradation activity of $29 \text{ mol}_{\text{H}_2\text{O}_2} \text{kg}_{\text{cat}}^{-1} \text{h}^{-1}$ was observed. Catalytic activity towards H_2O_2 degradation was seen to increase to a value of $113 \text{ mol}_{\text{H}_2\text{O}_2} \text{kg}_{\text{cat}}^{-1} \text{h}^{-1}$ when using 1 g of 4 wt% H_2O_2 , before plateauing when a higher volume, 3.0 g of 4 wt% H_2O_2 was added to the decan-1-ol solvent. With this plateau ascribed to the ability of H_2O_2 to catalyse the oxidation of Pd, as previously reported by Choudhary *et al.*,⁶⁴ with Pd^{2+}

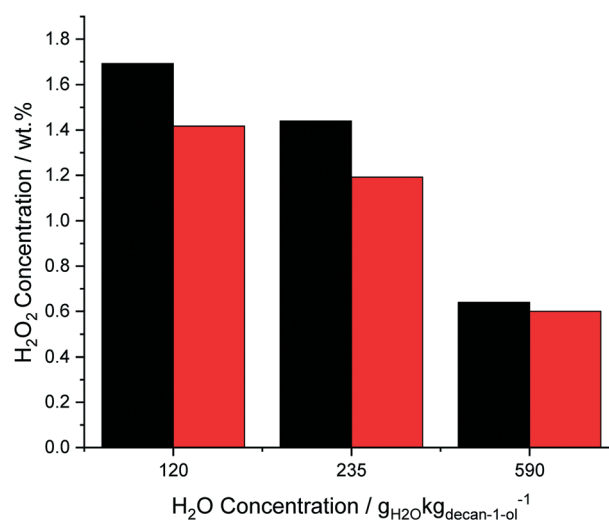


Fig. 3 Calculation of the H_2O_2 concentration in a mixture of decan-1-ol and water (black bars) and the separated water phase (red bars). H_2O_2 synthesis reaction conditions: 5% AuPd/C (0.01 g), total pressure (580 psi), H_2/O_2 (0.5), 1200 rpm, 8.5 g total solvent (decan-1-ol + H_2O), 25 °C, 30 min.



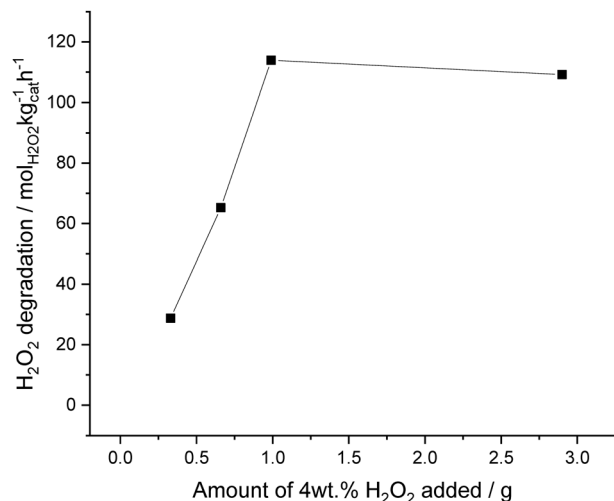


Fig. 4 Catalytic activity of a 5% AuPd/C catalyst towards H₂O₂ degradation with increasing amounts of aqueous 4 wt% H₂O₂. H₂O₂ synthesis reaction conditions: 5% AuPd/C (0.01 g), total pressure (580 psi), H₂/O₂ (0.5), 1200 rpm, 8.5 g total solvent decan-1-ol + X g 4 wt% H₂O₂, 25 °C, 30 min.

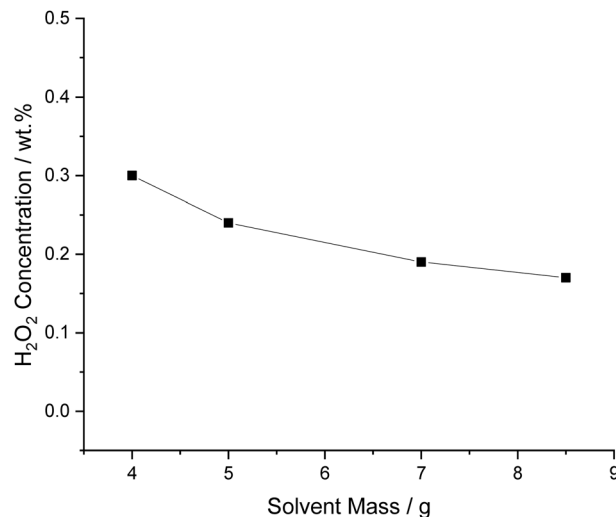


Fig. 5 The effect of total solvent mass on catalytic activity towards H₂O₂ synthesis. H₂O₂ synthesis reaction conditions: 5% AuPd/C (0.01 g), total pressure (580 psi), H₂/O₂ (0.5), 1200 rpm, X g total solvent (46 g_{H₂O} kg_{decan-1-ol}⁻¹), 25 °C, 30 min.

species known to be far less active towards H₂O₂ degradation than Pd⁰.^{66,67} The observed degradation activity, even at low amounts of H₂O₂ suggests that there is still some contact between catalyst and H₂O₂, which may be expected given the shear forces that result from high stirring speed used in this study it is promising that the amount of H₂O₂ degraded is relatively low. Indeed, it should be noted that the degradation activity observed using the proposed solvent system is far less than that previously reported over the same catalyst when using a miscible, H₂O/methanol solvent system, under identical reaction conditions (352 mol_{H₂O₂} kg_{cat}⁻¹ h⁻¹), although there are clear differences in H₂ solubility between H₂O/methanol solvent systems and those used within this study.³

The effect of solvent mass, while maintaining the mass of the 5% AuPd/C catalyst at 0.01 g, was next investigated (Fig. 5). As expected these results demonstrate that it is possible to enhance the concentration of H₂O₂ by decreasing the total solvent mass, this is mainly due to a dilution effect, producing the same amount of H₂O₂ in a smaller volume and increasing H₂ partial pressure relative to the solvent, due to increased reactor head space.

The effect of varying catalyst mass from 0.005 to 0.04 g, whilst keeping the solvent mass constant at 8.5 g, was next investigated (Fig. 6). It can be seen that with increasing mass of catalyst, H₂O₂ concentration increases in a non-linear manner, to a value of 0.25 wt% when using 0.02 g of catalyst, beyond which the increase in H₂O₂ concentration is far less pronounced. It is likely that the observed plateau in H₂O₂ concentration can be attributed to a combination of factors; (i) limitations associated with diffusion of reactant gas; (ii) the inability of the decan-1-ol to retain the catalyst forcing a higher concentration of catalyst into the aqueous phase, thus further increasing contribution of H₂O₂ degradation.

Time-on-line analysis was next carried out, with the vast majority of H₂O₂ seen to be produced over 30 minutes (0.17 wt%), although a steady rise in H₂O₂ concentration is observed over 60 minutes (0.19 wt%) (Fig. 7). Beyond 60 minutes there is a minor decrease in H₂O₂ concentration, presumably, this is due to a depletion in reagent gas availability, in particular, H₂ and the rate of H₂O₂ degradation exceeding that of H₂O₂ synthesis, with similar observations previously reported by Crole *et al.* in a range of solvents.² However, it is promising that H₂O₂ concentrations can be generally retained, even at extended reaction times.

In an attempt to further enhance H₂O₂ concentration, optimised conditions were combined from the previous experiments carried out above (Fig. 2–7); 0.02 g catalyst, 4 g

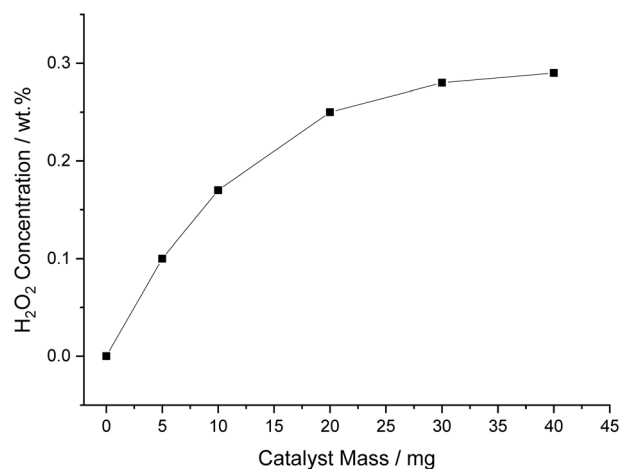


Fig. 6 The effect of catalyst mass on catalytic activity towards the direct synthesis of H₂O₂. H₂O₂ synthesis reaction conditions: 5% AuPd/C (X mg), total pressure (580 psi), H₂/O₂ (0.5), 1200 rpm, 8.5 g total solvent (46 g_{H₂O} kg_{decan-1-ol}⁻¹), 25 °C, 30 min.



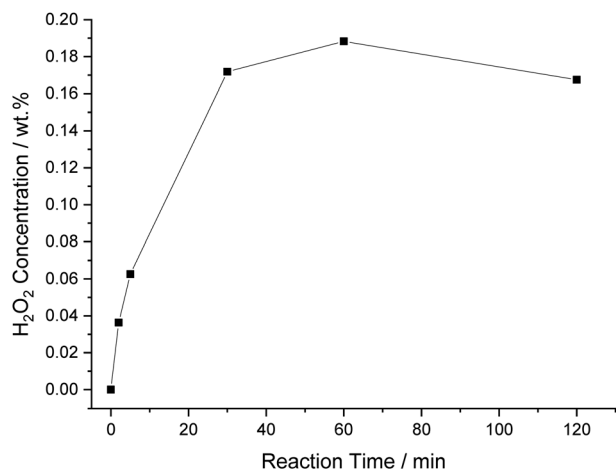


Fig. 7 The effect of reaction time on catalytic activity towards the direct synthesis of H₂O₂. H₂O₂ synthesis reaction conditions: 5% AuPd/C (0.01 g), total pressure (580 psi), H₂/O₂ (0.5), 1200 rpm, 8.5 g total solvent (46 g_{H₂O} kg_{decan-1-ol}⁻¹), 25 °C, X min.

total solvent with 46 g_{H₂O} kg_{decan-1-ol}⁻¹ and a reaction time of 30 minutes. It can be seen (Table 2, entry 2) that when the direct synthesis reaction was carried out with a total reactant gas pressure of 580 psi (H₂:O₂ = 0.5) it resulted in an H₂O₂ concentration of 0.45 wt%, over 2.5 times greater than that observed over non-optimised conditions (0.17 wt%). Further increasing total reaction pressure to 700 psi, while maintaining optimised reaction conditions (Table 2, entry 3) is observed to result in a 4-fold increase in H₂O₂ concentration (0.81 wt%) over standard conditions.

Finally, with the plateau in H₂O₂ concentration, previously observed (Fig. 7) we carried out a series of sequential H₂O₂ direct synthesis reactions under our optimised reaction conditions (Fig. 8). We observe a steady increase in H₂O₂ concentration up to 1.9 wt% after 5 sequential reactions.

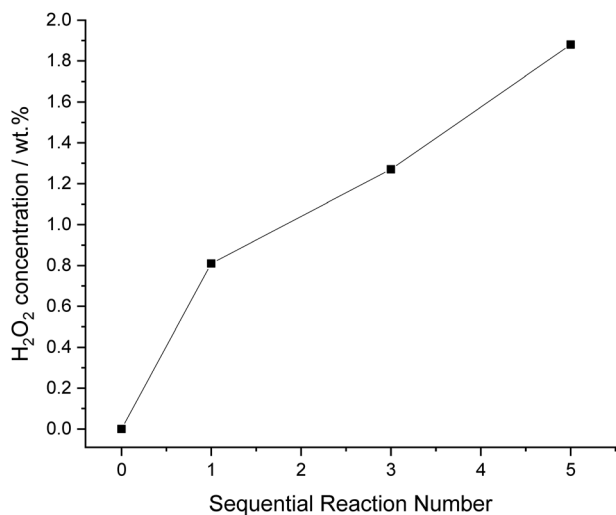


Fig. 8 Sequential H₂O₂ synthesis reactions, under optimised reaction conditions using a 5% AuPd/C catalyst. H₂O₂ synthesis reaction conditions: 5% AuPd/C (0.02 g), total pressure (700 psi), H₂/O₂ (0.5), 1200 rpm, 4 g total solvent (46 g_{H₂O} kg_{decan-1-ol}⁻¹), 25 °C, 30 min.

Although a limited volume of H₂O₂ is reported (0.16 ml of 1.9 wt% H₂O₂) at low productivities, the concentration achieved highlights the advantages of using a bi-phasic solvent for the direct synthesis of H₂O₂. If facile separation of the organic and aqueous phases can be achieved, the H₂O₂ concentration is comparable to that achieved in the initial stages of the current indirect method of industrial H₂O₂ production, prior to the use of multiple distillation steps to raise H₂O₂ concentrations to exceed ~70 wt%.³⁶

Conclusion

In this paper the direct synthesis of H₂O₂ from H₂ and O₂ over a 5% AuPd/C catalyst has been investigated using a solvent system containing decan-1-ol and water. As a result of the preference for the catalyst to be retained in the hydrophobic, organic component, thus limiting contact between the synthesised H₂O₂ and catalyst a significant improvement in catalytic efficacy is observed, compared to the use of a miscible solvent mixture. Through optimisation of the reaction conditions, and assuming facile separation of the organic and aqueous solvent, we demonstrate that it is possible to reach concentrations of H₂O₂ comparable to that produced in the initial stages of H₂O₂ production, on an industrial scale, with a H₂O₂ concentration of 1.9 wt% reported. Perhaps more importantly we demonstrate the feasibility of a bi-phasic solvent system in allowing simultaneous reaction and extraction, minimising H₂O₂ degradation rates, resulting in increased concentrations of H₂O₂. We consider that this work represents a promising basis for further exploration of a wider set of solvents and catalysts for use in the direct synthesis of H₂O₂. In particular we believe that, given the high desirability for a continuous production of H₂O₂, this approach would lend itself well to a flow regime.

Conflicts of interest

The authors declare no conflict of interests.

Acknowledgements

The authors wish to acknowledge the financial support of and research discussion with Solvay S. A.

References

- 1 A. Santos, R. J. Lewis, G. Malta, A. G. R. Howe, D. J. Morgan, E. Hampton, P. Gaskin and G. J. Hutchings, *Ind. Eng. Chem. Res.*, 2019, **58**, 12623–12631.
- 2 D. A. Crole, S. J. Freakley, J. K. Edwards and G. J. Hutchings, *Proc. R. Soc. London, Ser. A*, 2016, **472**, 20160156.
- 3 S. J. Freakley, R. J. Lewis, D. J. Morgan, J. K. Edwards and G. J. Hutchings, *Catal. Today*, 2015, **248**, 10–17.
- 4 T. Deguchi and M. Iwamoto, *J. Catal.*, 2011, **280**, 239–246.
- 5 E. N. Ntainjua, M. Piccinini, S. J. Freakley, J. C. Pritchard, J. K. Edwards, A. F. Carley and G. J. Hutchings, *Green Chem.*, 2012, **14**, 170.



- 6 J. Edwards, B. Solsona, P. Landon, A. Carley, A. Herzing, C. Kiely and G. Hutchings, *J. Catal.*, 2005, **236**, 69–79.
- 7 M. Piccinini, E. Ntainjua, J. K. Edwards, A. F. Carley, J. A. Moulijn and G. J. Hutchings, *Phys. Chem. Chem. Phys.*, 2010, **12**, 2488–2492.
- 8 V. V. Krishnan, A. G. Dokoutchaev and M. E. Thompson, *J. Catal.*, 2000, **196**, 366–374.
- 9 R. Burch and P. R. Ellis, *Appl. Catal., B*, 2003, **42**, 203–211.
- 10 R. J. Lewis and G. J. Hutchings, *ChemCatChem*, 2019, **11**, 298–308.
- 11 R. E. Brooks and S. B. Moore, *Cellulose*, 2000, **7**, 263–286.
- 12 C. Samanta, *Appl. Catal., A*, 2008, **350**, 133–149.
- 13 P. Landon, P. J. Collier, A. F. Carley, D. Chadwick, A. J. Papworth, A. Burrows, C. J. Kiely and G. J. Hutchings, *Phys. Chem. Chem. Phys.*, 2003, **5**, 1917–1923.
- 14 C. M. Piqueras, J. García-Serna and M. J. Cocero, *J. Supercrit. Fluids*, 2011, **56**, 33–40.
- 15 T. Moreno, J. García-Serna and M. J. Cocero, *Green Chem.*, 2010, **12**, 282–289.
- 16 Q. Chen and E. J. Beckman, *Green Chem.*, 2007, **9**, 802–808.
- 17 F. Moseley and P. N. Dyer, *US Pat.*, 4336240, 1982.
- 18 I. T. Horváth, *Acc. Chem. Res.*, 1998, **31**, 641–650.
- 19 M. Kawakami, Y. Ishiuchi, H. Nagashima, T. Tomita and Y. Hiramatsu, *US Pat.*, 5399334, 1995.
- 20 Q. Liu, J. C. Bauer, R. E. Schaak and J. H. Lunsford, *Appl. Catal., A*, 2008, **339**, 130–136.
- 21 S. Melada, F. Pinna, G. Strukul, S. Perathoner and G. Centi, *J. Catal.*, 2006, **237**, 213–219.
- 22 V. Paunovic, V. V. Ordonsky, V. L. Sushkevich, J. C. Schouten and T. A. Nijhuis, *ChemCatChem*, 2015, **7**, 1161–1176.
- 23 E. J. Beckman and J. Supercrit, *Fluids*, 2004, **28**, 121–191.
- 24 J. V. H. d'Angelo and A. Z. Francesconi, *J. Chem. Eng. Data*, 2001, **46**, 671–674.
- 25 M. S. Wainwright, T. Ahn, D. L. Trimm and N. W. Cant, *J. Chem. Eng. Data*, 1987, **32**, 22–24.
- 26 Z. Laughrey, E. Bear, R. Jones and M. A. Tarr, *Ultrason. Sonochem.*, 2001, **8**, 353–357.
- 27 R. J. Lewis, K. Ueura, Y. Fukuta, S. J. Freakley, L. Kang, R. Wang, Q. He, J. K. Edwards, D. J. Morgan, Y. Yamamoto and G. J. Hutchings, *ChemCatChem*, 2019, **11**, 1673–1680.
- 28 T. Pospelova and N. Kobozev, *Russ. J. Phys. Chem.*, 1961, **35**, 584–587.
- 29 E. N. Ntainjua, M. Piccinini, J. C. Pritchard, J. K. Edwards, A. F. Carley, J. A. Moulijn and G. J. Hutchings, *ChemSusChem*, 2009, **2**, 575–580.
- 30 S. Abate, P. Lanzafame, S. Perathoner and G. Centi, *Catal. Today*, 2011, **169**, 167–174.
- 31 S. Melada, F. Pinna, G. Strukul, S. Perathoner and G. Centi, *J. Catal.*, 2005, **235**, 241–248.
- 32 E. N. Ntainjua, M. Piccinini, J. C. Pritchard, Q. He, J. K. Edwards, A. F. Carley, J. A. Moulijn, C. J. Kiely and G. J. Hutchings, *ChemCatChem*, 2009, **1**, 479–484.
- 33 J. K. Edwards, B. Solsona, E. N. Ntainjua, A. F. Carley, A. A. Herzing, C. J. Kiely and G. J. Hutchings, *Science*, 2009, **323**, 1037–1041.
- 34 S. J. Freakley, Q. He, J. H. Harrhy, L. Lu, D. A. Crole, D. J. Morgan, E. N. Ntainjua, J. K. Edwards, A. F. Carley, A. Y. Borisevich, C. J. Kiely and G. J. Hutchings, *Science*, 2016, **351**, 965–968.
- 35 N. M. Wilson, J. Schröder, P. Priyadarshini, D. T. Bregante, S. Kunz and D. W. Flaherty, *J. Catal.*, 2018, **368**, 261–274.
- 36 H. Li, B. Zheng, Z. Pan, B. Zong and M. Qiao, *Front. Chem. Sci. Eng.*, 2018, **12**, 124–131.
- 37 Q. Liu and J. H. Lunsford, *Appl. Catal., A*, 2006, **314**, 94–100.
- 38 Y. Kawase, Y. Isaka, Y. Kuwahara, K. Mori and H. Yamashita, *Chem. Commun.*, 2019, **55**, 6743–6746.
- 39 Y. Isaka, Y. Kawase, Y. Kuwahara, K. Mori and H. Yamashita, *Angew. Chem., Int. Ed.*, 2019, **58**, 5402–5406.
- 40 X. Chen, Y. Kuwahara, K. Mori, C. Louis and H. Yamashita, *J. Mater. Chem. A*, 2020, **8**, 1904–1910.
- 41 J. E. Romo, N. V. Bollar, C. J. Zimmermann and S. G. Wettstein, *ChemCatChem*, 2018, **10**, 4805–4816.
- 42 V. M. Blasucci, Z. A. Husain, A. Z. Fadhel, M. E. Donaldson, E. Vyhmeister, P. Pollet, C. L. Liotta and C. A. Eckert, *J. Phys. Chem. A*, 2010, **114**, 3932–3938.
- 43 X. Jin, J. Feng, H. Song, J. Yao, Q. Ma, M. Zhang, C. Yu, S. Li and S. Yu, *Green Chem.*, 2019, **21**, 3583–3596.
- 44 G.-H. Han, X. Xiao, J. Hong, K.-J. Lee, S. Park, J.-P. Ahn, K.-Y. Lee and T. Yu, *ACS Appl. Mater. Interfaces*, 2020, **12**, 6328–6335.
- 45 Z. Cheng, R. Lippi, C. E. Li, Y. Yang, L. Tang, S. Huang, W. J. Lee, S. Lim, X. Ma and J. Patel, *Ind. Eng. Chem. Res.*, 2019, **58**, 20573–20584.
- 46 R. J. Lewis, J. K. Edwards, S. J. Freakley and G. J. Hutchings, *Ind. Eng. Chem. Res.*, 2017, **56**, 13287–13293.
- 47 E. N. Ntainjua, M. Piccinini, J. C. Pritchard, J. K. Edwards, A. F. Carley, C. J. Kiely and G. J. Hutchings, *Catal. Today*, 2011, **178**, 47–50.
- 48 E. N. Ntainjua, J. K. Edwards, A. F. Carley, J. A. Lopez-Sanchez, J. A. Moulijn, A. A. Herzing, C. J. Kiely and G. J. Hutchings, *Green Chem.*, 2008, **10**, 1162.
- 49 P. Tian, L. Ouyang, X. Xu, C. Ao, X. Xu, R. Si, X. Shen, M. Lin, J. Xu and Y.-F. Han, *J. Catal.*, 2017, **349**, 30–40.
- 50 A. Cybula, J. B. Priebe, M.-M. Pohl, J. W. Sobczak, M. Schneider, A. Zielińska-Jurek, A. Brückner and A. Zaleska, *Appl. Catal., B*, 2014, **152–153**, 202–211.
- 51 X. Gong, R. J. Lewis, S. Zhou, D. J. Morgan, T. E. Davies, X. Liu, C. J. Kiely, B. Zong and G. J. Hutchings, *Catal. Sci. Technol.*, 2020, **10**, 4635–4644.
- 52 L. Ouyang, P.-F. Tian, G.-J. Da, X.-C. Xu, C. Ao, T.-Y. Chen, R. Si, J. Xu and Y.-F. Han, *J. Catal.*, 2015, **321**, 70–80.
- 53 C. M. Crombie, R. J. Lewis, D. Kovačič, D. J. Morgan, T. E. Davies, J. K. Edwards, M. S. Skjøth-Rasmussen and G. J. Hutchings, *Catal. Lett.*, 2020, DOI: 10.1007/s10562-020-03281-1.
- 54 J. K. Edwards, A. F. Carley, A. A. Herzing, C. J. Kiely and G. J. Hutchings, *Faraday Discuss.*, 2008, **138**, 225.
- 55 J. K. Edwards, A. Thomas, A. F. Carley, A. A. Herzing, C. J. Kiely and G. J. Hutchings, *Green Chem.*, 2008, **10**, 388.
- 56 S. Kanungo, V. Paunovic, J. C. Schouten and M. F. Neira D'Angelo, *Nano Lett.*, 2017, **17**, 6481–6486.



- 57 S. Kanungo, L. van Haandel, E. J. M. Hensen, J. C. Schouten and M. F. Neira d'Angelo, *J. Catal.*, 2019, **370**, 200–209.
- 58 J. Li, T. Ishihara and K. Yoshizawa, *J. Phys. Chem. C*, 2011, **115**, 25359–25367.
- 59 N. M. Wilson, P. Priyadarshini, S. Kunz and D. W. Flaherty, *J. Catal.*, 2018, **357**, 163–175.
- 60 A. V. Beletskaya, D. A. Pichugina, A. F. Shestakov and N. E. Kuz'menko, *J. Phys. Chem. A*, 2013, **117**, 6817–6826.
- 61 F. Menegazzo, P. Burti, M. Signoretto, M. Manzoli, S. Vankova, F. Boccuzzi, F. Pinna and G. Strukul, *J. Catal.*, 2008, **257**, 369–381.
- 62 S. Bo, R. Battino and E. Wilhelm, *J. Chem. Eng. Data*, 1996, **41**, 644.
- 63 N. Šegatin and C. Klofutar, *Monatsh. Chem.*, 2004, **135**, 241–248.
- 64 V. R. Choudhary, C. Samanta and T. V. Choudhary, *J. Mol. Catal. A: Chem.*, 2006, **260**, 115–120.
- 65 V. R. Choudhary, C. Samanta and P. Jana, *Appl. Catal., A*, 2007, **317**, 234–243.
- 66 A. G. Gaikwad, S. D. Sansare and V. R. Choudhary, *J. Mol. Catal. A: Chem.*, 2002, **181**, 143–149.
- 67 G. Blanco-Brieva, E. Cano-Serrano, J. M. Campos-Martin and J. L. G. Fierro, *Chem. Commun.*, 2004, 1184–1185.

